Sciknow Publications Ltd.
Open Journal of Mathematical Modeling
OJMMO 2013, 1(2):46-57
DOI: 10.12966/ojmmo.05.05.2013

The Non-linear Modeling of the Rotational Vibrations of the Electrically Charged Cloud of the Ice Crystals

Artur Wirowski*

Department of Structural Mechanics, Technical University of Lodz, Lodz, Poland

*Corresponding author: (artur.wirowski@p.lodz.pl)

Abstract – The paper presents the derivation of the non-linear model of the vibrations of the electrically charged cloud of the ice crystals. This problem is applicable as the mechanical basis of a theoretical model of the atmospheric optical phenomenon commonly known as "the miracle of the Sun". A large crystal rotation angles and a continuous distribution of charges on the surface of the crystals are included in deliberations. It is shown that the obtained equation of the non-linear model is the type of the equation φ^4. The numerical solutions are shown for some examples of the model parameter sets. They are compared with the solutions of the linear model available in the literature. Finally, the obtained theoretical results have been compared with the results of the observations of the atmospheric phenomenon called "the miracle of the Sun" available in the literature.

Keywords – The Miracle of the Sun, Finite Difference Method, Non-linear Vibrations, Duffing's Equation, Equation φ^4

1. Introduction

1.1. The motivation to take the research topic

The problem of the vibration analysis of the electrically charged cloud of rotating ice crystals is a new matter. This line of the research was initiated in the paper [1]. The author of this paper by using a model of the electrically charged cloud of the ice crystals, oscillating under the influence of wind forcing, explained dynamically changing optical properties of the medium, and consequently atmospheric optical phenomenon commonly known as the "miracle of the Sun". This work was completely innovative perspective on this phenomenon, different in relation to previously existing studies [3,4], whereas a more complete explanation of many optical observations [1,2]. In this paper we would only like to take care of the mechanical modeling of this phenomenon, completely detached from the optical part of it.

In the paper [1] the first simplified model of electrostatic interactions between the crystals was proposed. The total electric charge of the crystal was divided into three point charges located in the middle and the ends of the plate crystal. It was assumed that the crystals rotated at very small angles and the effect of air resistance was skipped. Therefore, as a result of modeling, a linear vibration model was obtained, which was next used to analyze the optical phenomenon of "the miracle of the Sun". The mechanical model proposed in [1] is presented in Section 3.3 as a comparative model.

This paper is the continuation of deliberations concerning the dynamic behaviour of the ice crystals, which were begun in work [1], involving the significant extension of the assumptions used then. The continuous distribution of the electric charge on the surface of the ice crystals, large crystal rotation angles and the rotational damping by the air resistance will be included in the considerations. As a result the non-linear mechanical model will be obtained, which in future may be used for a more accurate analysis of the optical phenomenon of "the miracle of the Sun".

1.2. The applied methods of the modelling of the dynamic behaviour of the discrete media

It was necessary to formulate the continuous model of the cloud of the ice crystals in order to find a mathematical description of the relationship between angles of crystals' rotations and time and location. The finite difference method was used, due to the specificity of the vibration problem. The equation of rotational motion written for a single *i-th* crystal will be the starting point for modeling. After the appropriate formulation of this equation in the discrete form, it will be possible to pass to the continuous model by using the finite difference method theorems. This will be shown in section 2.5.

1.3. The aim and the scope of the paper

The aim of this study is to formulate a non-linear continuous model of rotational vibrations of a cloud of the electrically charged ice crystals. It will take into account the continuous distribution of electric charge on the surface of the ice crystal, their large angular rotations and the influence of the air resistance on the rotating crystals. The work includes the derivation of one-dimensional non-linear equation of the rotational oscillations of such a cloud, and the analysis of the limits of applicability and accuracy of this model. The study shows that the equation which describes such oscillations has the nature of a wave equation based on the Duffing's equation. The obtained exemplary numerical solutions have been compared to the simplified model included in the paper [1]. The results have also been discussed in the context of the empirical analysis of the observation of the optical phenomenon of "the miracle of the Sun" presented in the work [1].

2. The modeling

2.1. The assumptions

Let us introduce the following modeling assumptions (Figure 1):

A homogeneous cloud of identical, electrically charged ice crystals is given,

The crystals have the shape of regular hexagonal plates, i.e. their height is negligibly small in comparison to other dimensions,

The gravitational force acting on every crystal is balanced by the force of air resistance acting on a crystal falling down uniformly,

The air resistance forces influencing the crystal rotation are linearly proportional to the linear velocity in the rotational motion,

The electric charge of the crystal is uniformly distributed on its surface,

We assume that the synchronization occurs between the crystals, i.e. the difference between the rotation of two adjacent crystals is negligible.

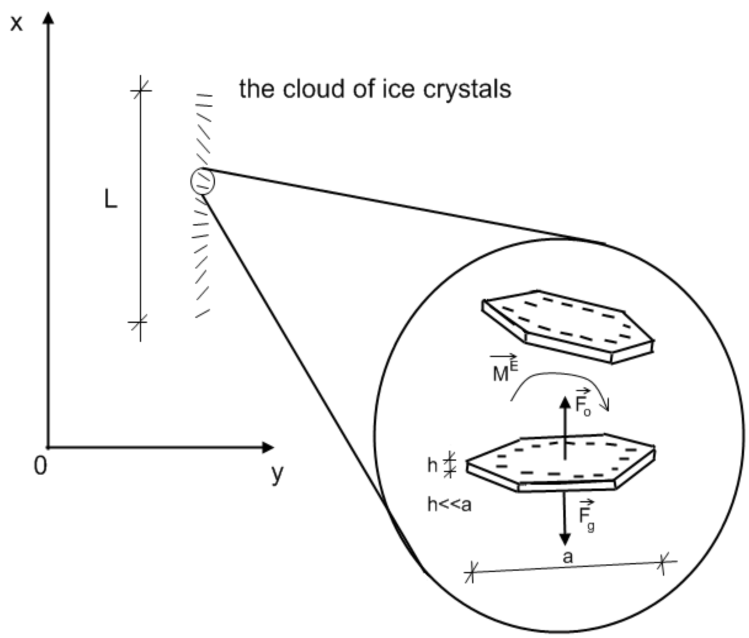

Figure 1. The schematic representation of the modeling assumptions. The individual regular hexagonal plate crystals are shown in enlargement.

2.2. The equation of the rotational motion of an individual crystal

$$\vec{M}_i = I_i \vec{\varepsilon}_i \quad (1)$$

where:

$I_i = \frac{5\sqrt{3}}{256} a_i^4 h_i \rho$ - the moment of inertia for the axis of crystal's rotation,

$\vec{M}_i$ - the total resultant moment acting on the *i-th* crystal,

$\vec{\varepsilon}_i$ - the angular acceleration in the rotational motion,

ρ - the density of ice.

Due to the continuous charge distribution on the crystals' surfaces, in the following modeling we consider the moments derived from the interaction between the appropriate surfaces of adjacent crystals. Then we can expand the resultant moment as (Figure 2):

$$\vec{M}_i = \int_{-\frac{a}{2}}^{\frac{a}{2}}\int_{-\frac{a}{2}}^{\frac{a}{2}} \vec{r}(\eta)\times\vec{F}_1(\eta,\xi_1)d\xi_1 d\eta + \int_{-\frac{a}{2}}^{\frac{a}{2}}\int_{-\frac{a}{2}}^{\frac{a}{2}} \vec{r}(\eta)\times\vec{F}_2(\eta,\xi_2)d\xi_2 d\eta + \int_{-\frac{a}{2}}^{\frac{a}{2}} \vec{r}(\eta)\times\vec{F}_R(\eta)d\eta + \vec{M}_i^E \tag{2}$$

where:

$\vec{r}(\eta)=[\eta,0]$ is a conductive vector of an infinitely small segment of the surface of the *i-th* crystal, i $\vec{F}_2(\eta,\xi_2)$ are the forces of the electrostatic interaction between the infinitely small segments of the surface of adjacent crystals respectively $d\xi_1$ and $d\eta$ in case of $\vec{F}_1(\eta,\xi_1)$ and $d\xi_2$ and $d\eta$ in case of $\vec{F}_2(\eta,\xi_2)$. $\vec{F}_R(\eta)$ is the force of air resistance acting on an infinitely small segment of the crystal's surface. The coordinates η, ξ_1 and ξ_2 are local coordinates, running respectively on the surfaces of the *i-th*, *i+1-th* and *i-1-th* crystal and adopting the values from -½ to ½ for the extreme edges of the crystal and *0* in the midst of each surface (Figure 2). $\vec{M}_i^E$ is the external forcing vibrations moment.

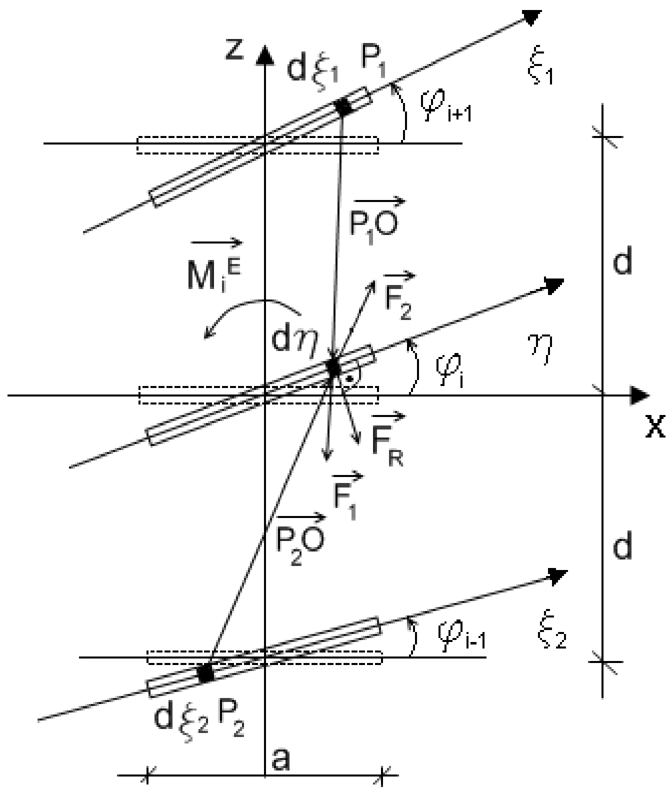

Figure 2. The electrostatic forces between the infinitely small segments of the surfaces of the analyzed crystals.

The resistance force, in accordance to the assumptions, is proportional to the linear velocity of segment $d\eta$, and forces $\vec{F}_1(\eta,\xi_1)$ and $\vec{F}_2(\eta,\xi_2)$ are Coulomb forces and therefore:

$$\vec{F}_1(\eta,\xi_1)=\frac{dq\cdot dq}{4\pi\varepsilon_r\varepsilon_0}\cdot\frac{\overline{P_1O}}{\left|P_1O\right|^3},\ \vec{F}_2(\eta,\xi_2)=\frac{dq\cdot dq}{4\pi\varepsilon_r\varepsilon_0}\cdot\frac{\overline{P_2O}}{\left|P_2O\right|^3}\ \vec{F}_R(\eta)=R\frac{\partial\vec{\phi}}{\partial t}\eta \tag{3}$$

where:

R is the coefficient of air resistance,

$\overline{P_1O} = \left[-d\sin\varphi_i - \xi_1\cos\Delta\varphi_{1i} + \eta, -d\cos\varphi_i - \xi_1\sin\Delta\varphi_{1i}\right]$ and

$\overline{P_2O} = \left[d\sin\varphi_i - \xi_2\cos\Delta\varphi_{2i} + \eta, d\cos\varphi_i + \xi_2\sin\Delta\varphi_{2i}\right]$

are vectors of beginnings and ends at the points P_1 and O respectively and at P_2 and O (Figure 2), which are the points of the analyzed segments of crystals' surfaces $d\xi_1, d\eta$ and $d\xi_2$.

$\Delta\varphi_1 = \varphi_{i+1} - \varphi_i$ and $\Delta\varphi_2 = \varphi_i - \varphi_{i-1}$ are the differences between the angles of crystals' rotations respectively for *i-th*, *i+1-th and i-1-th* crystal.

dq is the charge of the analyzed segment of the crystal's surface,

ε_r is the relative dielectric constant of air,

ε_0 is the dielectric constant of vacuum.

By substituting these relations into equation (2) and expanding the vector product we obtain:

$$\vec{M}_i = \frac{1}{4\pi\varepsilon_r\varepsilon_0}\sum_{\alpha=1,2}\int_{-\frac{a}{2}}^{\frac{a}{2}}\int_{-\frac{a}{2}}^{\frac{a}{2}}\frac{\eta_\alpha\left(\mp d\cos\varphi_i \mp \xi_\alpha\sin\Delta\varphi_{\alpha i}\right)}{\left(\left(\mp d\sin\varphi_i - \xi_\alpha\cos\Delta\varphi_{\alpha i} + \eta_\alpha\right)^2 + \left(\mp d\cos\varphi_i \mp \xi_\alpha\sin\Delta\varphi_{\alpha i}\right)^2\right)^{\frac{3}{2}}}\cdot(dq)^2 d\xi_\alpha d\eta - R\frac{\partial\vec{\varphi}_i}{\partial t}\int_{-\frac{a}{2}}^{\frac{a}{2}}\eta^2 d\eta + \vec{M}_i^E \tag{4}$$

Where in symbols "$\mp$","$\pm$" the upper operator corresponds to $\alpha = 1$, the lower one to $\alpha = 2$

The equation (4) may be subject to certain simplifications. Let us note, that due to the uniform charge distribution on the surface of each crystal, we have:

$$Q = \int_{-\frac{a}{2}}^{\frac{a}{2}} dq d\xi_\alpha = \int_{-\frac{a}{2}}^{\frac{a}{2}} dq d\eta, \alpha = 1,2 \tag{5}$$

Due to the assumption of the synchronization of the crystals, which means that the adjacent crystals are rotated by almost the same angles, we have:

$$\Delta\varphi_{\alpha i} << 1 \Rightarrow \sin\Delta\varphi_{\alpha i} = \Delta\varphi_{\alpha i}, \cos\Delta\varphi_{\alpha i} = 1 \tag{6}$$

Due to these relations, the equation (4) can be simplified after some transformations to the form:

$$\vec{M}_i = \frac{Q^2}{4\pi\varepsilon_r\varepsilon_0}\sum_{\alpha=1,2}\int_{-\frac{a}{2}}^{\frac{a}{2}}\int_{-\frac{a}{2}}^{\frac{a}{2}}\frac{\mp d\eta\cos\varphi_i \mp \Delta\varphi_{\alpha i}\eta\xi_\alpha}{\left(d^2 + (\eta - \xi_\alpha)^2 \pm 2d\cdot\xi_\alpha\sin\varphi_{i\pm1} \mp 2d\eta\sin\varphi_i\right)^{\frac{3}{2}}} d\xi_\alpha d\eta - \frac{Ra^3}{12}\frac{\partial\vec{\varphi}_i}{\partial t} + \vec{M}_i^E \tag{7}$$

2.3. *The derivation of the discrete equation of the rotational motion of the crystals*

Although the solution of double integrals (7) exists in the general case, it is very complicated. In view of the fact that it is also a discrete equation of the rotation angle, which subsequently will be subject of conversion into a continuous form, the use of the exact solutions of the equation (7) for this purpose is impossible. To solve the given problem we can find the approximate solution of double integrals (7) with a reasonable accuracy. We use the assumption of the synchronization of crystals, i.e. the fact that the differences between the rotation angles of adjacent crystals are relatively small. In this case, we may assume that the moment induced by the crystals' rotation by identical angles is independent of the moment induced by the symmetric and anti-symmetric components of the differences of the appropriate angles (Figure 3):

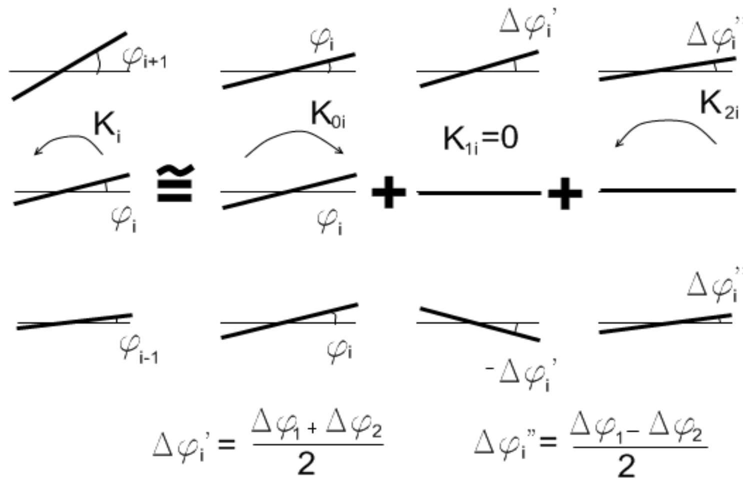

Figure 3. The assumption of superposition of the moments caused by crystals' rotation by identical angles and moments caused by the symmetric and antisymmetric components of the differences of the appropriate angles, which is described by (9).

Let us denote the integrals from equation (7) by $K_i(d,a,\varphi_i,\varphi_{i+1},\varphi_{i-1})$:

$$M_i = \frac{Q^2}{4\pi\varepsilon_r\varepsilon_0} K_i(d,a,\varphi_i,\varphi_{i+1},\varphi_{i-1}) + \frac{Ra^3}{12}\frac{\partial\varphi_i}{\partial t} + M_i^E \tag{8}$$

We assume, that the following superposition of the moments is true:

$$K_i(d,a,\varphi_i,\varphi_{i+1},\varphi_{i-1}) \cong K_{0i}(d,a,\varphi_i) + K_{1i}(d,a,\Delta\varphi_{\alpha i}) + K_{2i}(d,a,\Delta\varphi_{\alpha i}) \tag{9}$$

$$K_{0i}(d,a,\varphi_i) = K_i(d,a,\varphi_i,\varphi_{i+1},\varphi_{i-1})\Big|_{\substack{\varphi_{i+1}-\varphi_{i-1}=0 \\ \varphi_{i+1}-2\varphi_i+\varphi_{i-1}=0}}$$

$$K_{1i}(d,a,\Delta\varphi_{\alpha i}) = K_i(d,a,\varphi_i,\varphi_{i+1},\varphi_{i-1})\Big|_{\substack{\varphi_i=0 \\ \varphi_{i+1}-2\varphi_i+\varphi_{i-1}=0}}$$

$$K_{2i}(d,a,\Delta\varphi_{\alpha i}) = K_i(d,a,\varphi_i,\varphi_{i+1},\varphi_{i-1})\Big|_{\substack{\varphi_i=0 \\ \varphi_{i+1}-\varphi_{i-1}=0}}$$

The correctness and the accuracy of this assumption will be tested in later discussion. Let us calculate the moment $K_{0i}(d,a,\varphi_i)$. In this case the simplifications can be transformed (9) into:

$$\varphi_i = \varphi_{i+1} = \varphi_{i-1} \text{ and } \Delta\varphi_{\alpha i} = 0$$

Both integrals (7) give the same solution for $\alpha = 1$ and $\alpha = 2$ due to the symmetry of the task, so by denoting $\hat{d} = \frac{d}{a}$, we get:

$$K_{0i}(\hat{d},a,\varphi_i) = \frac{2}{a}\int_{-\frac{1}{2}}^{\frac{1}{2}}\int_{-\frac{1}{2}}^{\frac{1}{2}} \frac{-\hat{d}\eta\cos\varphi_i}{\left(\hat{d}^2 + 2\hat{d}(\eta-\xi_1)\sin\varphi_i + (\eta-\xi_1)^2\right)^{\frac{3}{2}}}\, d\xi_\alpha\, d\eta \tag{10}$$

In case $K_{1i}(d,a,\Delta\varphi_{\alpha i})$ we have:

$$\varphi_i = 0, \varphi_{i+1} = \Delta\varphi_i', \varphi_{i-1} = -\Delta\varphi_i', \Delta\varphi_{1i} = \Delta\varphi_i', \Delta\varphi_{2i} = -\Delta\varphi_i'$$

It can be proved that:

$$K_{1i}(d,a,\Delta\varphi_{\alpha i}) = 0 \tag{11}$$

due to the symmetry of the moments induced by the electrostatic forces from the upper and lower crystal, as it is shown in Figure 3.

For the remaining $K_{2i}(d,a,\Delta\varphi_{\alpha i})$ we have:

$$\varphi_i = 0, \varphi_{i+1} = \Delta\varphi_i'', \varphi_{i-1} = \Delta\varphi_i'', \quad \Delta\varphi_{\alpha i} = \Delta\varphi_i''$$

After the transformations and the substitutions, which are analogous to the ones performed in the calculation of K_0, we obtain:

$$K_{2i}\left(\hat{d},a,\Delta\varphi_i''\right)=\frac{2}{a}\int_{-\frac{1}{2}}^{\frac{1}{2}}\int_{-\frac{1}{2}}^{\frac{1}{2}}\frac{-\hat{d}\eta_1-\Delta\varphi_i''\eta\xi_1}{\left(\hat{d}^2+2\hat{d}\xi_1\Delta\varphi_i''+\left(\eta_1-\xi_1\right)^2\right)^{\frac{3}{2}}}d\xi_1 d\eta \tag{12}$$

We can calculate the integrals (10) and (12) in an accurate manner. By denoting respectively:

$$\tilde{d}_{+i}=\sqrt{\hat{d}^2+2\hat{d}\sin\varphi_i+1},\ \breve{d}_{+i}=\sqrt{1+\hat{d}\Delta\varphi_i''+\hat{d}^2},\ \check{d}_{+i}=\sqrt{\hat{d}(\hat{d}+\Delta\varphi_i'')}$$
$$\tilde{d}_{-i}=\sqrt{\hat{d}^2-2\hat{d}\sin\varphi_i+1},\ \breve{d}_{-i}=\sqrt{1-\hat{d}\Delta\varphi_i''+\hat{d}^2},\ \check{d}_{-i}=\sqrt{\hat{d}(\hat{d}-\Delta\varphi_i'')},$$

we get:

$$K_{0i}\left(\hat{d},a,\varphi_i\right)=-\frac{\hat{d}}{a}\cos\varphi_i\ln\frac{\left(\hat{d}\sin\varphi_i+1+\tilde{d}_{+i}\right)\left(\hat{d}\sin\varphi_i-1+\tilde{d}_{-i}\right)}{\left(\hat{d}\sin\varphi_i+\hat{d}\right)^2}-\frac{tg\varphi_i}{a}\left(\tilde{d}_{+i}+\tilde{d}_{-i}-2\hat{d}\right) \tag{13}$$

$$\begin{aligned}K_{2i}\left(\hat{d},a,\Delta\varphi_i''\right)=&\frac{\hat{d}}{a}\left(\frac{1}{4\left(\Delta\varphi_i''\right)^2}+\frac{\left(\Delta\varphi_i''\right)^2}{2}-1\right)\ln\left(\frac{\left(\hat{d}\Delta\varphi_i''+1+\breve{d}_{+i}\right)\left(\hat{d}\Delta\varphi_i''-1+\breve{d}_{-i}\right)}{\left(\hat{d}\Delta\varphi_i''+\check{d}_{+i}\right)\left(\hat{d}\Delta\varphi_i''+\check{d}_{-i}\right)}\right)+\\&+\frac{1}{a}\left(\frac{\Delta\varphi_i''}{2}+\frac{1}{2\Delta\varphi_i''}\right)\left(\check{d}_{+i}+\check{d}_{-i}-\breve{d}_{+i}-\breve{d}_{-i}\right)+\frac{1}{2a\hat{d}}\left(\check{d}_{+i}-\check{d}_{-i}\right)+\\&+\frac{\hat{d}sign\left(\Delta\varphi_i''\right)}{4a\left(\Delta\varphi_i''\right)^2}\ln\left(\frac{\left[\hat{d}\Delta\varphi_i''\check{d}_{+i}^{\,2}+\check{d}_{-i}^{\,2}\left(-1+sign\left(\Delta\varphi_i''\right)\breve{d}_{+i}\right)\right]\left[\hat{d}\Delta\varphi_i''\check{d}_{-i}^{\,2}+\check{d}_{+i}^{\,2}\left(1+sign\left(\Delta\varphi_i''\right)\breve{d}_{-i}\right)\right]}{\check{d}_{+i}^{\,2}\check{d}_{-i}^{\,2}\left(\hat{d}\Delta\varphi_i''+sign\left(\Delta\varphi_i''\right)\breve{d}_{-i}\right)\left(\hat{d}\Delta\varphi_i''+sign\left(\Delta\varphi_i''\right)\breve{d}_{+i}\right)}\right)\end{aligned} \tag{14}$$

Finally, the discrete equation of the crystals' rotation takes the form:

$$I_i\frac{\partial^2\varphi_i}{\partial t^2}-\frac{Q^2}{4\pi\varepsilon_r\varepsilon_0}\left(K_{0i}\left(\hat{d},a,\varphi_i\right)+K_{2i}\left(\hat{d},a,\Delta\varphi''_i\right)\right)+\frac{Ra^3}{12}\frac{\partial\varphi_i}{\partial t}=-M_i^E \tag{15}$$

Next we have performed a numerical experiment involving 1000 different sets of test parameters *a, d,* φ, $\Delta\varphi_1$, $\Delta\varphi_2$ randomly selected, in order to verify the accuracy of the previously adopted assumption (9), and consequently the accuracy of the equation (15). The model parameters have been selected from the physically possible ranges:

$$a\in\left(0.5mm,10mm\right),\ \hat{d}\in\left(0.5,50\right),\ \varphi\in\left(-60°,60°\right),\ \Delta\varphi_1\in\left(-0.2°,0.2°\right),\ \Delta\varphi_2\in\left(-0.2°,0.2°\right) \tag{16}$$

The following parameters have been calculated numerically for each randomly selected combination of input parameters: g $K_i\left(\hat{d},a,\varphi_i,\varphi_{i+1},\varphi_{i-1}\right)$, $K_{0i}\left(\hat{d},a,\varphi_i\right)$ and $K_{2i}\left(\hat{d},a,\Delta\varphi_{\alpha i}\right)$ and the approximation error has been calculated according to the formula:

$$\Delta X_i=\left|\frac{K_i-(K_{0i}+K_{2i})}{K_i}\right|\cdot 100\% \tag{17}$$

As a result of the numerical experiment, it has been found that the arithmetic mean of the absolute value of errors calculated according to the formula (17), associated with the approximation, (9) is only 0.03‰. The largest error occurs when the parameters of φ and $\Delta\varphi_i''$ are similar. However, due to the assumption of the synchronization of crystals, $\Delta\varphi_i''$ is a small angle, and this situation does not occur in practice. Therefore, we can conclude that for given ranges of input data (16), the assumption (9) is practically satisfied in an accurate manner.

2.4. The approximation of the discrete equation of the motion

The obtained equation (15) is a very complicated formula of the discrete parameters φ_i and $\Delta\varphi''_i$ Let us notice that in order to be able to transform it to a continuous model using the finite difference method formulas, the coefficients K_{0i} and K_{2i} must depend on the parameters φ_i and $\Delta\varphi''_i$ in the simplest possible way.

Hence, the series of graphs illustrating the correlation between the coefficients K_{0i} and K_{2i} and the parameters φ_i and $\Delta\varphi''_i$ have been performed. The Figures 4 and 5 have been made for the selected allowable parameters of the model defined by (16):

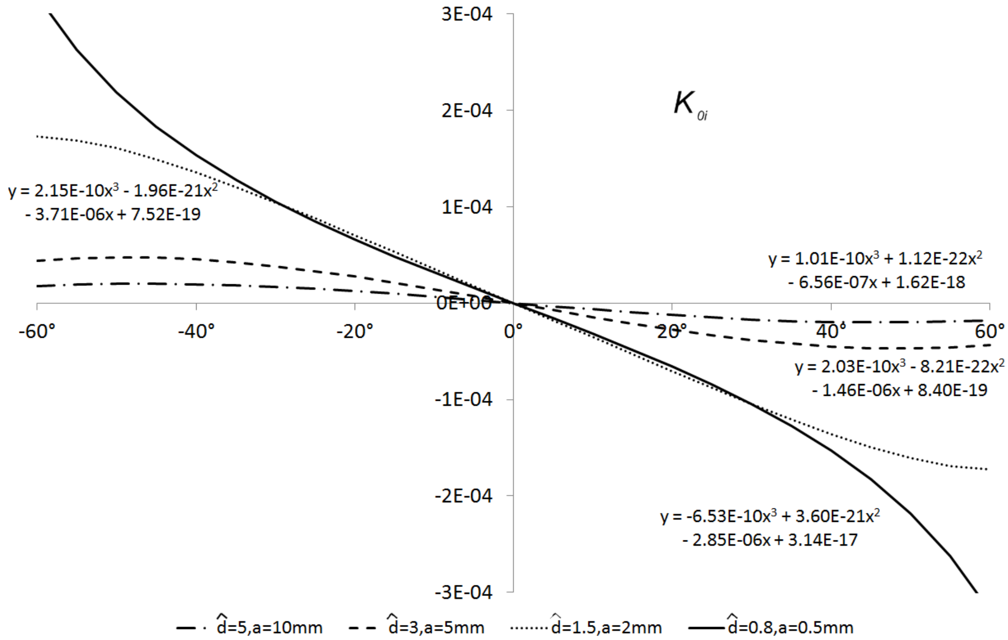

Figure 4. The dependency of the coefficients K0i from the discrete parameter fi for the selected combinations of the parameters a and $\hat{d}$.

We apply the linear approximation of the coefficient K_{2i}, which is the exact approximation in the range of angles. $\Delta\varphi'' \in (-0.2°, 0.2°)$.

$$K_{2i} = \kappa_1(\hat{d}, a)\Delta\varphi_i'' \tag{18}$$

In the case of K_{0i} we get good results in the range of angles $\varphi \in (-60°, 60°)$ after using a polynomial approximation of the 3rd order. It is worth noting that the polynomial approximating K_{0i} has the form (Figure 4):

$$K_{0i} = \kappa_2(\hat{d}, a)\varphi_i^3 - \kappa_3(\hat{d}, a)\varphi_i \tag{19}$$

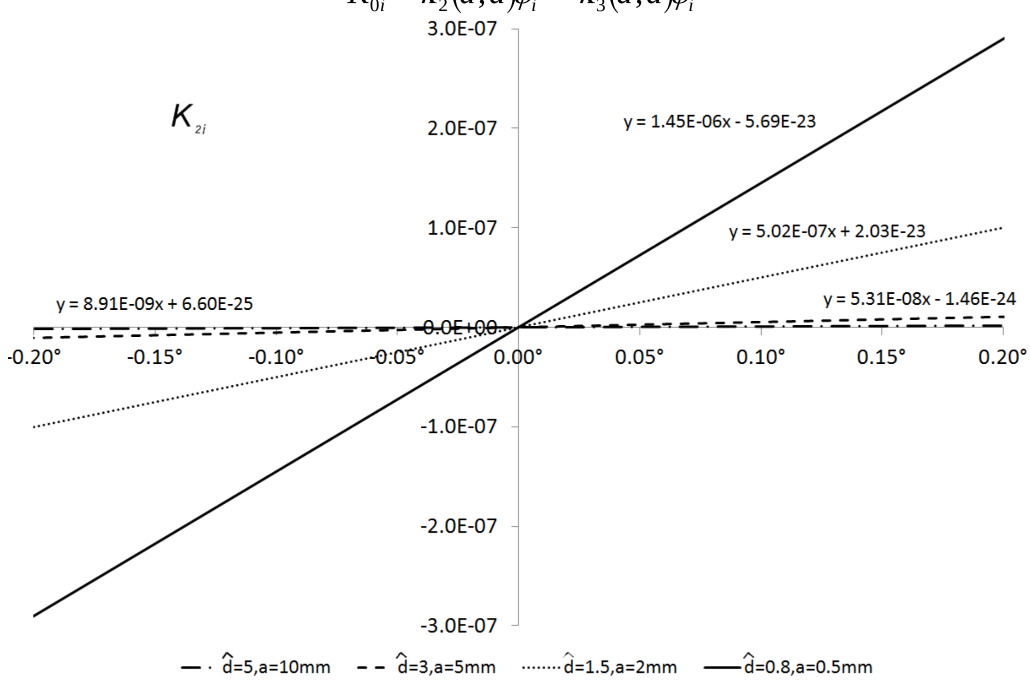

Figure 5. The dependency of the coefficients K2i from the discrete parameter Df"i for the selected combinations of the parameters a and $\hat{d}$.

The remaining coefficients of the 3-rd order development are equal nearly to zero due to the specific shape of the graph K_{0i}

and they can be ignored, regardless of the combination of the other parameters of the model. We can also note that the approximation coefficients κ_1 and κ_3 are positive, regardless of the parameters of the model, and the following inequality is satisfied:

$$\kappa_3(\hat{d},a) > \kappa_1(\hat{d},a)$$

The coefficient κ_2 may take both positive and negative values, depending on the parameter $\hat{d}$. If the inequality $\hat{d} =< 1$ is satisfied, the coefficient κ_2 assumes the negative values, if the strong inequality $\hat{d} >> 1$ is satisfied, the coefficient κ_2 assumes the positive values. In the case when $\hat{d} > 1$, but $\hat{d} \approx 1$, the sign of the coefficient κ_2 can be different and it also depends on the other parameters of the model. As a result of the polynomial approximation of the coefficients K_{0i} and K_{2i} the following equation is obtained:

$$I_i \frac{\partial^2 \varphi_i}{\partial t^2} - \frac{Q^2}{16\pi\varepsilon_r\varepsilon_0}\left(\kappa_2(\hat{d},a)\varphi_i^3 - \kappa_3(\hat{d},a)\varphi_i + \kappa_1(\hat{d},a)\Delta\varphi_i''\right) + \frac{Ra^3}{12}\frac{\partial \varphi_i}{\partial t} = -M_i^E \tag{20}$$

where $\kappa_1(\hat{d},a) = \frac{180}{\pi} K_{2i}(\hat{d},a,\Delta\varphi_i'')\Big|_{\Delta\varphi''=\frac{\pi}{180}}$, $\kappa_2(\hat{d},a) = \frac{36}{\pi^3}\left(K_{0i}(\hat{d},a,\varphi_i)\Big|_{\varphi=\frac{\pi}{3}} - 2K_{0i}(\hat{d},a,\varphi_i)\Big|_{\varphi=\frac{\pi}{6}}\right)$,

$$\kappa_3(\hat{d},a) = \frac{1}{\pi}\left(K_{0i}(\hat{d},a,\varphi_i)\Big|_{\varphi=\frac{\pi}{3}} - 8K_{0i}(\hat{d},a,\varphi_i)\Big|_{\varphi=\frac{\pi}{6}}\right)$$

The equation (20) has coefficients, which are independent of the discrete parameters φ_i and $\Delta\varphi''_i$ and it can be used to construct the continuous model of the vibrations of the cloud of the ice crystals.

2.5. The continuous model of the vibrating cloud

Next we transform the discrete equation (20) to a continuous form in order to build the continuous model of the vibrating cloud. We will use the finite difference method formulas:

$$\varphi = \varphi_i \quad \text{and} \quad \frac{\partial^2 \varphi}{\partial x^2} = \frac{\varphi_{i+1} - 2\varphi_i + \varphi_{i-1}}{d^2} \tag{21}$$

Let us note, that $\Delta\varphi''_i = \frac{\varphi_{i+1} + \varphi_{i-1}}{2}$ (Figure 3). By substituting the relations (21) into the equation (20) and after appropriate transforming and grouping the components, we get:

$$\mu^2 \frac{\partial^2 \varphi(x,t)}{\partial t^2} + \psi^2 \frac{\partial \varphi(x,t)}{\partial t} - \alpha^2 \frac{\partial^2 \varphi(x,t)}{\partial x^2} + \beta^2 \varphi(x,t) + \gamma(\varphi(x,t))^3 = -M^E(x,t) \tag{22}$$

where

$$\mu^2 = \frac{5\sqrt{3}\pi\varepsilon_r\varepsilon_0 h\rho a^4}{16Q^2}, \psi^2 = \frac{4\pi\varepsilon_r\varepsilon_0 Ra^3}{3Q^2}, \alpha^2 = \frac{d^2}{2}\kappa_1(\hat{d},a), \beta^2 = \kappa_3(\hat{d},a) - \kappa_1(\hat{d},a), \gamma = \kappa_2(\hat{d},a).$$

The equation (22) describes the vibrations of the cloud of the electrically charged ice crystals in the continuous form. It takes into account the continuous distribution of the electric charge on the surface of the crystals, their rotation by large angles, the external forcing and the air resistance. This equation describes the case of the non-linear vibrations and it is known in the literature as *the equation* φ^4.

3. The exemplary analysis of the problem of the non-linear vibrations of the cloud of the ice crystals

3.1. The assumptions

The equation (22) has analytical solutions only for some specific boundary conditions, as the example of φ^4 *equation* [5] [6]. Finding, at least approximate, numerical solutions and their visualization is a difficult task, due to the nature of the possible solutions, which can be chaotic, harmonic and unlimited in some areas too. Therefore we make a simplification for an easier visualization of the solutions of this equation. Let us note, that if we are interested in the solutions for the large angles φ for which the following condition is satisfied:

$$\varphi >> \Delta\varphi'' \tag{23}$$

this strong inequality is true:

$$K_0\left(\hat{d},a\right) >> K_2\left(\hat{d},a\right) \tag{24}$$

Then we can reduce the equation (22) to an ordinary differential equation, which is called Duffing's equation:

$$\mu^2 \frac{d^2\varphi(t)}{dt^2} + \psi^2 \frac{d\varphi(t)}{dt} + \beta^2\varphi(t) + \gamma(\varphi(t))^3 = -M^E(t) \tag{25}$$

By omitting the member $\alpha^2 \frac{\partial^2\varphi(x,t)}{\partial x^2}$ from the equation (22), this equation has lost its wavy character, because it is only a function of time. In physical terms, it means no propagation of the vibration of the crystals in the direction of the *x*-axis. However the solutions of the equation (25) allow us for the visualization of the potential types of the vibrations, which are the base for the wavy motion of the cloud of the ice crystals, more generally described by the equation (22). The equation (25) has the exact solutions as a Jacobi function [7]. They may be of either harmonic or chaotic type, which depends on the parameters of the equation and the initial-boundary conditions.

If the parameter $\gamma < 0$, the equation (25) as an example of Duffing's equation, leads to the solutions known as „hard-spring" model. In this case, the force of the interaction between the crystals grows faster than linearly for the large angles of the rotation of the crystals (Figure 4 - solid line). This occurs, when the crystals are close enough, i.e. $\hat{d} \approx< 1$. The „hard-spring" solutions could be chaotic for a relatively large amplitude of the external forcing vibrations moment. There may be also periods when the vibrations are harmonic or quasi-harmonic. The vibrations are always limited, therefore in any case the angle of the rotation of the crystals cannot be greater than 90°.

If the parameter $\gamma > 0$, the equation (25) leads to the solutions known as „soft-spring" model. In this case the force of the interaction between the crystals grows slower than linearly for the large angles of the rotation of the crystals (Figure 4 - dashed lines). This occurs when the crystals are appropriately distant from one another, i.e. $\hat{d} \approx> 1$. The „soft-spring" solutions are harmonic for a relatively small amplitude of the external forcing vibrations moment. If the external moment is sufficiently large, the vibrations grow in the theoretically unlimited way. It means that the rotation of the crystals can be greater than 180°. This situation leads to the disorder of the synchronization between the crystals.

3.2. The sample solution of the problem of the vibration cloud of the ice crystals

Below we show the selected examples of the solutions of the equation (25). We assume a sinusoidal external forcing vibrations moment described by the following formula:

$$M^E(t) = \Gamma \sin(\omega t) \tag{26}$$

and the initial conditions corresponding to the slight initial deflection:

$$\varphi(0) = 10°, \left.\frac{d\varphi(t)}{dt}\right|_{t=0} = 0 \tag{27}$$

Furthermore, in all cases the same values of physical and material constants have been assumed:

$$r=916.7\ kg/m^3,\ \varepsilon_0 = 8.8542\cdot10^{-12}\frac{F}{m},\ \varepsilon_r = 1.00054$$

We have adopted the following parameters of the model:

	a)	*b)*	*c)*	*d)*
d [mm]	*0.4*	*0.4*	*15*	*15*
a [mm]	*0.5*	*0.5*	*5*	*5*
h[mm]	*0.01*	*0.01*	*0.1*	*0.1*
R[kg/s]	*3 ·104*	*3 ·104*	*3.17 ·104*	*3.17 ·104*
Q[C]	*9.29 ·10-10*	*9.29 ·10-10*	*2.94 ·10-7*	*2.94 ·10-7*
Γ *[Nm]*	*3.40 ·10-5*	*1.50 ·10-5*	*5.00 ·10-9*	*5.00 ·10-5*
ω *[Hz]*	*5.00 ·10^{-2}*	*5.00 ·10^{-2}*	*5.00 ·10^{-2}*	*5.00 ·10^{-2}*

Table1. The adopted sets of the model parameters.

The cases a) and b) lead to the "hard-spring" model, and the cases c) and d) – to the "soft-spring" model. The cases a) and b) and c) and d) respectively differ from one another only in the amplitude of the external forcing vibrations moment.

For the above set of parameters, the following coefficients of the equation (25) have been obtained:

	a)	*b)*	*c)*	*d)*
μ^2 *[Nms²]*	$1.00 \cdot 10^{-4}$	$1.00 \cdot 10^{-4}$	$1.00 \cdot 10^{-4}$	$1.00 \cdot 10^{-4}$
ψ^2 *[Nms]*	$1.50 \cdot 10^{-7}$	$1.50 \cdot 10^{-7}$	$5.00 \cdot 10^{-7}$	$5.00 \cdot 10^{-7}$
β^2 *[Nm]*	$1.40 \cdot 10^{-6}$	$1.40 \cdot 10^{-6}$	$1.46 \cdot 10^{-6}$	$1.46 \cdot 10^{-6}$
γ *[Nm]*	$6.53 \cdot 10^{-10}$	$6.53 \cdot 10^{-10}$	$-2.03 \cdot 10^{-10}$	$-2.03 \cdot 10^{-10}$
Γ *[Nm]*	$3.40 \cdot 10^{-5}$	$1.50 \cdot 10^{-5}$	$5.00 \cdot 10^{-9}$	$5.00 \cdot 10^{-5}$

Table 2. The coefficients of the equation (25) for different sets of the model parameters.

The following charts shows the deflection of the crystals as a function of time. They show the diversity of the potential solutions of the equation (25) (Figure 6):

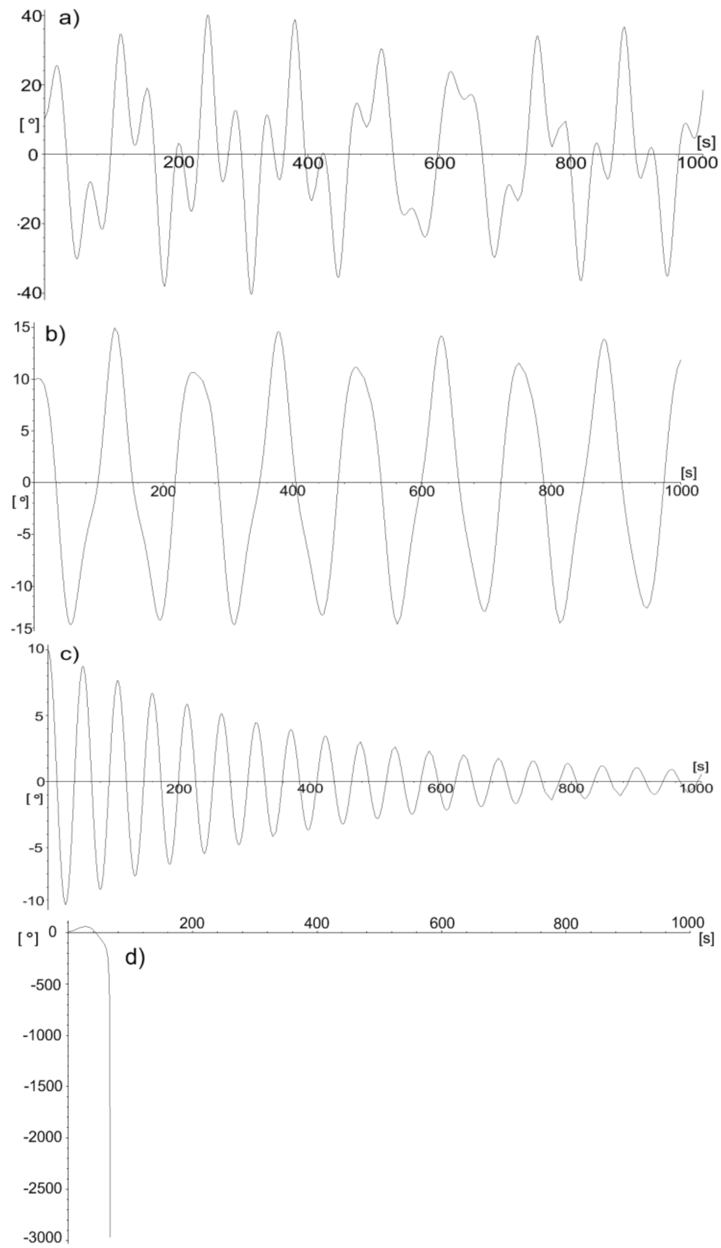

Figure 6. The sample diagrams of the deflection of the crystals versus time corresponding to the different parameters of the model: a) the "hard-spring" model – the chaotic vibrations, b) the „hard-spring" model – the quasi-harmonic vibrations c) the „soft-spring" model – the damped harmonic vibrations, d) the „soft-spring" model – the theoretically unlimited vibrations (the full turn of the crystal)

After analyzing the above diagrams, we can conclude that:

- the solution of the equation (25) and consequently the equation (22) can be very diversified, depending on the model parameters and the initial-boundary conditions: they can be either harmonic, quasi-harmonic or chaotic,
- the period of vibrations depends on the amplitude,
- in case of the "hard-spring" model the vibrations with smaller amplitude are more regular than the vibrations with the greater amplitude,
- in case of the "soft spring" model the rotation of the crystals can be greater than 180°, so it leads to the disorder of the synchronization between the crystals.

3.3. The simplified model

The previously existing model of the rotational vibrations of the electrically charged cloud of the ice crystals was presented in [1]. It assumed that:

- A homogeneus cloud of electrically charged identical ice crystals is given;
- Crystal rotation is the result of their electrostatic interactions;
- The difference between the rotation of two adjacent crystals is negligible;
- The gravitational force, operating on each crystal, is balanced by the force of air resistance acting on the uniformly falling crystal;
- We ignore the influence of air resistance on the rotating crystals;
- For simplification the electric charge of a crystal is reduced to 3 charges located at the ends and in the middle of the ice crystal;
- We assume that the crystals have the form of thin plates with negligible thickness;
- The difference between the rotation of two adjacent crystals is negligible;
- The crystals rotate only by small angels relative to the horizontal position;

By transforming the equation of the rotational motion of a single crystal the discrete equation, analogous to the formula (15) from this work, was obtained in [1] in a relatively simple way:

$$-I_i\varepsilon_i + \frac{kQ^2a^2}{d}\left(\frac{\varphi_{i+1} - 2\varphi_i + \varphi_{i-1}}{d^2}\right) + M_i^E = 0 \tag{28}$$

Next, by using the finite difference method we transform the formula (29) to a continuous model of the cloud:

$$\frac{1}{v^2}\frac{\partial^2\varphi}{\partial t^2} - \frac{\partial^2\varphi}{\partial x^2} = \theta M(x,t) \tag{29}$$

where: $v^2 = \dfrac{256kQ^2}{45\sqrt{3}hd\rho l^2}, \theta = \dfrac{9d}{kQ^2l^2}, I = \dfrac{5\sqrt{3}}{256}l^4h\rho$

We assume, analogously to assumption in Section 3.2, the sinusoidal external forcing vibrations moment and the initial-boundary conditions in the form:

$$\varphi(x,t)\big|_{t=0} = 0, \left.\frac{\partial\varphi(x,t)}{\partial t}\right|_{t=0} = 0, \ \varphi(x,t)\big|_{x=0} = 0, \ \varphi(x,t)\big|_{x=L} = 0 \tag{30}$$

We obtain the solution:

$$\varphi(x,t) = A_0 \cdot \left[\sin\left(\frac{\pi v t}{L}\right)\omega L - \sin(\omega t)\pi v\right]\sin\left(\frac{\pi}{L}x\right) \tag{31}$$

This solution is purely harmonic, regardless of the assumed parameters of the model.

4. The Conlusions and the Summary

As a result of the modelling, the continuous non-linear equations of the vibrations of a cloud of ice crystals (22) has been obtained. When we compare the numerical solution obtained from the equation reduced to Duffing's equation (25) and other solutions of this equation, which are known from the literature [7], with the solution of the simplified model (31) and the optical observations of the phenomenon known as "miracle of the Sun" described in [1], we can see that:

1. The solutions of non-linear model may be harmonic, quasi-harmonic, chaotic or unlimited as opposed to only harmonic nature of the simplified model solutions. The analysis of the observations of the phenomenon included in [1] indicated a generally irregular nature of the oscillations with some periods of very good harmonization. The description of the non-linear model and especially "hard-spring" solutions corresponds to this experiment to a big extent.
2. The period of the vibration in a non-linear model depends on the amplitude of the forcing strength and is related to the

amplitude of the vibration. In paper [1], the observed vibrations of type A and B, which differ in amplitude, were described. The greater amplitude of the vibrations were always characterized with a greater period of the vibrations. This coincidence could not be explained by the linear model.

3. In paper [1], it was also observed that the vibration of type A of a smaller amplitude, was characterized with a higher regularity, than the one of type B of a greater amplitude. When we compare it to the Figure 6ab ("hard-spring" model), we can notice that the vibrations become more chaotic with an increase in amplitude,.

In conclusion, we can say that the mechanical model of the non-linear vibration of the electrically charged cloud of the ice crystals, received in this study, allows us for a much better explanation of many of the observed characteristics of the optical phenomenon called " the miracle of the Sun" than the model proposed in [1].

In subsequent studies the author plans to expand the proposed model by taking into account the pencil crystals of a large height. This model would allow us to describe two-dimensional problems.

References

[1] A. Wirowski, Modeling of the Phenomenon Known as “the Miracle of the Sun” as the Reflection of Light from Ice Crystals Oscillating Synchronously, Journal of Modern Physics, Vol. 3 No. 3, 2012,

[2] J. De Marchi, The Immaculate Heart, Farrar, Straus and Young, New York, 1952,

[3] M. Hope-Ross, S. Travers, D. Mooney, Solar Retinopathy Following Religious Rituals, British Journal of Ophthalmology, Vo. 72, No. 12, 1988,

[4] S. Campbell, The Miracle of the Sun at Fátima, Journal of Meteorology, Vol. 14, No. 142, 1989

[5] A.A. Soliman, H.A. Abdo,: New Exact Solutions of Non-linear Variants of the RLW, the PHI-four and Boussinesq Equations Based on Modified Extended Direct Algebraic Method, International Journal of Non-linear Science, Vol. 7 (2009), No. 3,

[6] A. Bekir,: New Exact Travelling Wave Solutions for Regularized Long-wave, Phi-Four and Drinfeld-Sokolov Equations, International Journal of Non-linear Science, Vol. 6 (2008), No. 1,

[7] I. Kovacic, M.J. Brennan, The Duffing Equation, Non-linear Oscillators and their Behaviour, John Wiley & Sons, 2011.